Eur. Phys. J. B **43**, 399–403 (2005)
DOI: 10.1140/epjb/e2005-00070-2

THE EUROPEAN PHYSICAL JOURNAL B

Quantum interference in nanotube electron waveguides

Linfeng Yang[1,2,a], Jiangwei Chen[2], Huatong Yang[2], and Jinming Dong[2]

[1] Department of Mathematics and Physics, Zhongyuan University of Technology, Zhengzhou 450007, China
[2] National Laboratory of Solid State Microstructures and Department of Physics, Nanjing University, Nanjing 210093, China

Received 28 December 2003 / Received in final form 30 September 2004
Published online 15 March 2005 –

Abstract. We have calculated the quantum conductance of single-walled carbon nanotube (SWNT) waveguide by using a tight binding-based Green's function approach. Our calculations show that the slow conductance oscillations as well as the fast conductance oscillations are manifestations of the intrinsic quantum interference properties of the conducting SWNTs, being independent of the defect and disorder of the SWNTs. And zigzag type tubes do not show the slow oscillations. The SWNT electron waveguide is also found to have distinctly different transport behavior depending on whether or not the length of the tube is commensurate with a $(3N + 1)$ rule, with N the number of basic carbon repeat units along the nanotube length.

PACS. 73.22.-f Electronic structure of nanoscale materials: clusters, nanoparticles, nanotubes, and nanocrystals – 73.23.-b Electronic transport in mesoscopic systems – 73.63.Fg Nanotubes

Carbon nanotubes have induced a great deal of interests since their discovery in 1991 by Iijima et al. [1]. One of their most fascinating aspects is that their electronic and transport properties are directly and sensitively related to their geometry structures, which are uniquely determined by the circumference vector, $\vec{c} = n_1\vec{a_1} + n_2\vec{a_2}$, where $\vec{a_1}$ and $\vec{a_2}$ are graphite sheet lattice translation vectors. The pair of integer numbers (n_1, n_2) defines the radius and chirality of each tube. Tubes of $(n, 0)$ and (n, n) are nonchiral, while others are chiral with their hexagonal carbon atoms are arranged in a helical fashion. All (n, n) armchair nanotubes are metals, and the (n_1, n_2) tubes with the radii >3.5 Å are semimetallic if $(n_1 - n_2)$ is a nonzero multiple of three. The rest are semiconductors with band gaps that scale roughly as the reciprocal of the tube radius [2–5].

Carbon nanotubes can be either metals or semiconductors, depending on their helicity and diameter. This remarkable property suggests that it may be possible in the future to construct an all-carbon nanotube-based nanoelectronic devices. To explore this exciting possibility, there has been a considerable amount of theoretical and experimental researches on the electronic properties of the carbon nanotubes. Progress has been rapid and a number of prototypical devices for laboratory studies have already been created. Their ability to sustain a ballistic electronic current has been experimentally demonstrated [6–9], providing the basis for using nanotubes as efficient metallic wires.

The behavior of traditional electronic devices can be understood in term of the classical diffusive motion of electrons. As the size of a device becomes comparable to the electron coherence length, the quantum interference between electron waves becomes increasingly important, leading to dramatic changes in the device properties. This classical-to-quantum transition in the device behavior suggests the possibility of using quantum coherence in nanometer-sized electronic elements. Molecular electron devices are promising candidates for realizing such device elements because the electronic motion in molecules is inherently quantum mechanical and it can be modified by well defined chemistry. An other example of a coherent electronic devices is the Fabry-Perot electron resonator based on individual SWNTs with near-perfect ohmic contacts to electrodes [7,8], in which the nanotubes act as coherent electron wave guides with the resonant cavity formed between the two nanotube-electrode interfaces, and the coupling between the two propagating modes caused by electron scattering at the nanotube-electrode interfaces is important.

Within the Landauer formalism, the ballistic conductance of a perfect system is proportional to the number of conducting channels at the Fermi energy. In the case of an isolated metallic SWNT, two bands derived from the π-bonding and π-antibonding orbitals between neighboring carbon atoms cross at the Fermi level (E_F), leading to a perfect transmission in the case of ideal electrical contact, and corresponding two units of quantum conductance $G = 2G_0$. Of importance in a transport experiment is the coupling of the SWNT to metallic leads, and in

[a] e-mail: lfyzz@yahoo.com.cn

the case of imperfect electrical contacts, the elastic scattering on interfaces affects the transmission coefficients and thereby reduces the conductance, which then is no longer precisely quantized. For SWNTs, the conductance $G = T \times 2G_0 = \frac{4Te^2}{h}$ with transmission probability up to $T \sim 0.5{-}0.6$ has been observed in transport measurements [10,11].

Recently, however, a highly transparent contact of $T \sim 1$ has been made in the individual metallic SWNT at low temperature [8], which presents a clear evidence of quantum transport as expected from theory. In addition, rapid conductance oscillations are observed to be superimposed on slow fluctuation background. The authors ascribed the fast oscillations to the confinement-induced discrete "particle-in-a-box" electronic states, the additional slow modulated envelope of the fast oscillations and the deep dip to the localized states due to defects or chemical species adsorbed on SWNTs. However, the defects on SWNT contradicts the fact of the maximum quantum conductance limit $2G_0$ observed in their experiments, which is implication of the perfect structure for the carbon nanotubes.

In this paper, we have calculated the quantum conductance of the near transparent contacted SWNTs by using a tight binding-based Green's function approach that is particularly suitable for realistic calculations of the electronic transport properties in extended systems [12]. Our calculations show that conducting SWNTs with perfect ohmic contacts contributes two conductance channels as predicted by previous theoretical works; In the fine contacted systems, the slow oscillated fluctuation background is an intrinsic quantum coherent properties in all metallic nanotube resonators except zigzag ones, which are independent of the localized states due to the imperfections. Both rapid and slow conductance fluctuations are quantum interference phenomena, but the former comes from linear terms in the energy dispersion relations of metallic nanotubes, while the latter from nonlinear ones [13]. And the ratio between the slow and fast oscillation periods relate only to the nanotube length and the gate-voltage used in experiments, independent of the coupling strength between nanotube and the electric contact. And the SWNT electron waveguide is found to have distinctly different transport behavior depending on wether or not the length of the tube is commensurate with a $(3N+1)$ rule, with N the number of basic carbon repeat units along the nanotube length.

The geometrical structure under consideration is composed of two leads(left and right) plus SWNT, with all three parts being metallic SWNTs of the same chirality, which can be described by a tight-binding model with one π electron per atom. The tight-binding Hamiltonian of the system is written as

$$H = -V_{pp\pi} \sum_{\langle ij \rangle} a_i^\dagger a_j + \text{h.c.}, \tag{1}$$

where the sum over i, j is restricted to the nearest-neighbor site, and $V_{pp\pi} = 2.75$ eV [14]. Within this theory, the defect-free nanotubes have complete electron-hole symmetry with their Fermi levels at zero. The layers of carbon atoms between left and right leads are chosen to be 813 for armchair tubes and 939 for zigzag tubes (the length of nanotube $L = 200$ nm) and half of that to show the length effect. For simplicity, On-site energies are set to zero, all nearest-neighbor hopping parameters are assumed to be $V_{pp\pi}$ except those at contacts, which are taken to be $\alpha \cdot V_{pp\pi}$ with $0 < \alpha < 1$. Consequently, electrons will be slightly scattered at interfaces and the system behave like a Fabry-Perot type nanotube electron waveguide.

A fundamental result in the theory of electronic transport is that the conductance G of the SWNT electron waveguide can be obtained by the Landauer formula

$$G = \frac{2e^2}{h}\mathcal{T}, \tag{2}$$

with $\mathcal{T}$, the transmission function, which can be expressed in terms of the Green's functions of SWNT and the coupling coefficients of the SWNT to the leads [15,16]:

$$\mathcal{T} = \text{Tr}(\Gamma_L G_C^r \Gamma_R G_C^a), \tag{3}$$

here $G_C^{\{r,a\}}$ are the retarded and advanced Green's functions of the SWNT, and $\Gamma_{\{L,R\}}$ are the coupling of the SWNT to the leads. The Green's function for the SWNT can be explicitly written as

$$G_C(\epsilon) = (\epsilon - H_C - \Sigma_L - \Sigma_R)^{-1}, \tag{4}$$

where $\Sigma_L = h_{LC}^\dagger g_L h_{LC}$ and $\Sigma_R = h_{RC} g_R h_{RC}^\dagger$ are the self-energy terms due to the semi-infinite leads, h_{LC} and h_{RC} are the coupling matrices that will be nonzero only for adjacent points between the SWNT and the leads, and $g_{\{L,R\}} = (\epsilon - H_{\{L,R\}})^{-1}$ are the Green's functions of the leads. The coupling functions $\Gamma_{\{L,R\}}$ can be easily obtained by the following formula [17]

$$\Gamma_{\{L,R\}} = i\left[\Sigma_{\{L,R\}}^r - \Sigma_{\{L,R\}}^a\right]. \tag{5}$$

Following the method of references [13,18], we obtain $\Sigma_L = h_{LC}^\dagger \overline{T}$ and $\Sigma_R = h_{CR} T$. Here T and $\overline{T}$ are the appropriate transfer matrices, which are easily computed from the Hamiltonian matrix elements via an iterative procedure [12,18]

$$T = t_0 + \tilde{t}_0 t_1 + \tilde{t}_0 \tilde{t}_1 t_2 + \ldots + \tilde{t}_0 \tilde{t}_1 \tilde{t}_2 \ldots t_n, \tag{6}$$

$$\overline{T} = \tilde{t}_0 + t_0 \tilde{t}_1 + t_0 t_1 \tilde{t}_2 + \ldots + t_0 t_1 t_2 \ldots \tilde{t}_n, \tag{7}$$

where t_i and $\tilde{t}_i$ are defined via the recursion formulas:

$$t_i = (I - t_{i-1}\tilde{t}_{i-1} - \tilde{t}_{i-1} t_{i-1})^{-1} t_{i-1}^2, \tag{8}$$

$$\tilde{t}_i = (I - t_{i-1}\tilde{t}_{i-1} - \tilde{t}_{i-1} t_{i-1})^{-1} \tilde{t}_{i-1}^2, \tag{9}$$

and

$$t_0 = (\epsilon - H_C)^{-1} h_{LC}^\dagger, \tag{10}$$

$$\tilde{t}_0 = (\epsilon - H_C)^{-1} h_{CR}. \tag{11}$$

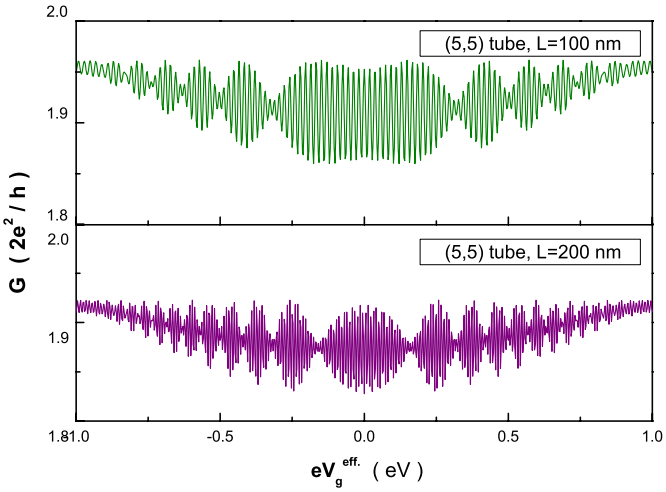

Fig. 1. Conductance G (in units of G_0) of (5,5) armchair SWNT vs. effective gate-voltage $eV_g^{(eff.)}$ with $L = 100$ nm, $\alpha = 0.70$ (up); and $L = 200$ nm, $\alpha = 0.70$ (down).

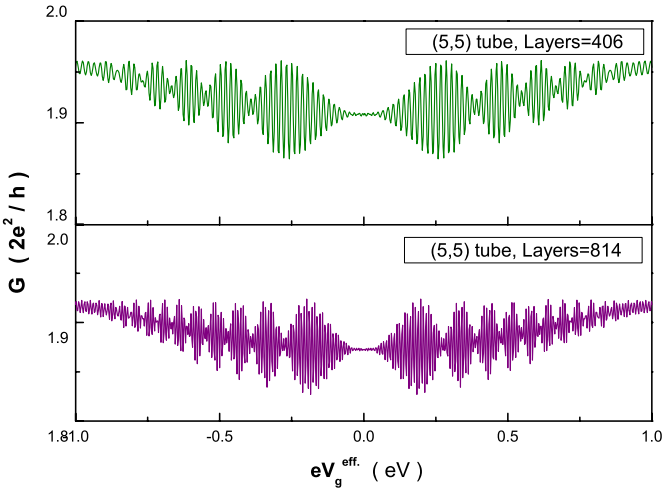

Fig. 2. Conductance G (in units of G_0) of (5,5) armchair SWNT vs. effective gate-voltage $eV_g^{(eff.)}$ with $N = 406$ layers, $\alpha = 0.70$ (up); and $N = 814$ layers, $\alpha = 0.70$ (down).

The process is repeated until $t_n, \tilde{t}_n \leq \delta$ with δ arbitrarily small [12,18].

We have calculated the conductance of the electron waveguides of metallic SWNTs at zero temperature and zero bias. The conductance G versus the Fermi energy E_F (E_F can be changed by the applied effective gate-voltage $V_g^{eff\cdot}$, hence we use $eV_g^{eff\cdot}$ to represent the Fermi energy E_F relative to charge neutrality energy point.) for the (5,5) tube are shown in Figure 1 to Figure 2 and (9,0) tube shown in Figure 3, respectively, which illustrate several characteristics shared by all metallic SWNTs. First, all the metallic SWNTs electron waveguides exhibit pronounced fast oscillations with the maximum conductance approaching $2G_0$, the result fast conductance oscillations period $\Delta E \approx 0.0093$ eV for the resonator length $L = 200$ nm (the length in the experiment) and $\Delta E \approx 0.019$ eV for $L = 100$ nm coincides very well with that of the experiment and previous theoretical prediction [8,19], showing the metallic SWNTs really have two channels and the fast conductance oscillations period is proportional to L^{-1} which is the manifestation of electron scattering occurring only at the SWNT-electric contact interface and passing through SWNT ballistically. Second, the conductance oscillation behavior shown in the $G \sim eV_g^{eff\cdot}$ plots is quite different between the armchair and zigzag SWNT electron resonators, slowly oscillating envelope of the fast oscillations with the Fermi energy $eV_g^{eff\cdot}$ is very clear in Figures 1 and 2. but none in Figure 3. In fact, all metallic SWNT resonators have the slow oscillation background except the zigzag ones. As the chiral angle θ is bigger enough to make the slow oscillation period ΔE_0 be smaller than the measured energy interval ΔE in the experiments, the slow oscillation background will be observed. Third, the ratio of the slow oscillation period and fast oscillation period is independent of the coupling strength of the SWNT and electric contact, but is relevant to the SWNT length L (see Figs. 1 and 2). Forth, all (3N+1)-unit length electron resonators(for armchair tubes considered here, a repeat unit is defined as two carbon layers along the length of the nanotube), the oscillations tends to disappear near the charge neutrality energy point. This result can be understood that the corresponding length of SWNT is integer multiple of the electron wave-length, which is $3a$ ($a = \sqrt{3}a_{cc}$, $a_{cc} = 1.42$ Å is the length of carbon bond) at this energy point. The interfacial scattering will be weak as the standing wave condition is satisfied, so will the conductance oscillations. The (3N+1) rule result also functions in the conductance of carbon nanotubes based magnetic tunnel junctions [20]. Fifth, as there is no impurity and disorder in our calculation, so the slow and fast oscillations is the property of intrinsic quantum interference. The defect and disorder on carbon nanotube will of course effect the structure and transport properties of SWNT [21–23], we also calculated the conductance of the system with defect and disorder in the perfect contacted case, however, no regular slow oscillations appeared, indicating the slow oscillation is independent of the defect or disorder [24]. In addition to the fast and slow oscillations described above, we can see from Figure 1 to Figure 3 that the fast and slow oscillations superimposed on a slower oscillation fluctuations too, which reveals that the conductance of SWNT resonators have more subtle structure, which are resulted from the electrical contacts coupling and higher nonlinear term in energy dispersion relation.

The fast oscillations can be understood by the discrete 'particle-in-a box' electronic states, and the fast oscillation period is determined by [7,8,19] $\Delta E \approx (\frac{dE}{dk})\Delta k = \frac{hV_F}{2L} \approx \frac{(1.68\ \text{eVnm})}{L}$. $\Delta E = 0.0084$ eV for $L = 200$ nm and $\Delta E = 0.0168$ eV for $L = 100$ nm. In reference [8] the gate-voltage period of the fast conductance oscillations is $\Delta V = 0.2$ eV with its effective gate-voltage coefficient $\alpha = 0.05$, the experimental fast oscillations period $\Delta E = 0.01$ eV match our calculations results $\Delta E = 0.093$ eV. To understand the slow oscillations, we need use the energy

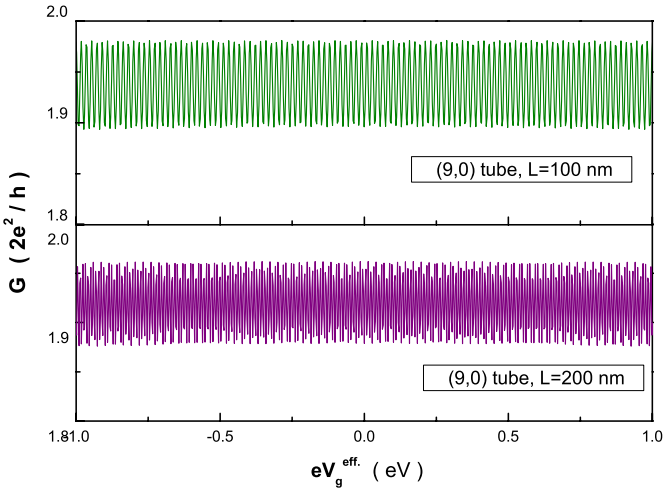

Fig. 3. Conductance G (in units of G_0) of (9,0) armchair SWNT vs. effective gate-voltage $eV_g^{(eff.)}$ with $L = 100$ nm, $\alpha = 0.70$ (up); and $L = 200$ nm, $\alpha = 0.70$ (down).

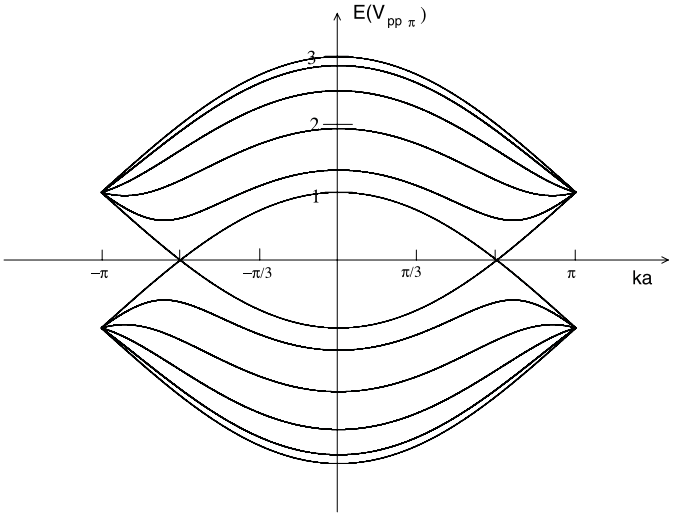

Fig. 4. Energy dispersion relation of (5,5) SWNT around Fermi energy.

dispersion relation near Fermi energy (see Figs. 4 and 5 for representatives)

$$eV_g^{eff\cdot} = \pm V_{pp\pi}\left\{1 - 2\cos\left(\frac{ka}{2}\right)\right\},$$

(for armchair metallic SWNTs)

$$eV_g^{eff\cdot} = \pm 2V_{pp\pi}\sin\left(\frac{\sqrt{3}ka}{4}\right).$$

(for zigzag metallic SWNTs). (12)

Up to second order of $eV_g^{eff\cdot}$ and $V_F = \frac{\sqrt{3}aV_{pp\pi}}{2\hbar}$, the two forward propagating wave vectors k_1 and k_2 are obtained [13]:
For the armchair metallic SWNT resonators

$$k_1 \doteq \frac{2\pi}{3a} + \frac{eV_g^{eff\cdot}}{\hbar V_F} + \frac{\sqrt{3}a}{12}\left(\frac{eV_g^{eff\cdot}}{\hbar V_F}\right)^2, \quad (13)$$

$$k_2 \doteq -\frac{2\pi}{3a} + \frac{eV_g^{eff\cdot}}{\hbar V_F} - \frac{\sqrt{3}a}{12}\left(\frac{eV_g^{eff\cdot}}{\hbar V_F}\right)^2. \quad (14)$$

For the zigzag metallic SWNT resonators

$$k_1 \equiv k_2 \doteq \frac{eV_g^{eff\cdot}}{\hbar V_F}. \quad (15)$$

Since the electrical contacts and SWNT coupling interaction, the electronic wave packets will be partially scattered into another channel on the interfaces. The unscattered parts of one channel are independent of those of another channel. However, the scattered parts of two channels are coupled, and quantum interference may take place between them. For perfect contacted SWNTs, the two channel are independent and the conductance of the system is $2G_0 = \frac{4e^2}{h}$. In the near-perfect contacted case of SWNT electron resonators, the quantum interference between electrical wave of one channel will result in conductance fast oscillations: A wave injected from a channel will be transmitted to the same channel, forming a series of transmitted partial waves, each of which differs from the previous one by two extra reflections plus a round trip between the barriers. The phase difference between two neighbor partial waves is $2k_1L$ (or $2k_2L$), and the phase change due to gate-voltage variation will be $\delta\varphi \doteq \frac{2Le\Delta V_g^{eff\cdot}}{\hbar V_F}$. This relation can well explain the experimental results [7,8]. And quantum interference among the scattered parts of two channels will induce slow oscillated background. Scattered wave incoming from one channel can be transmitted into another channel, the phase difference between two neighbor partial wave pertaining to different channels is $2(k_1 - k_2)L$, and the phase change coming from gate-voltage variation is $\delta\varphi \doteq \frac{2\sqrt{3}La}{3}(\frac{e}{\hbar V_F})^2 V_g^{eff\cdot}\Delta V_g^{eff\cdot}$, result in a slow oscillations background with the rapid oscillations superimposed on it. And the slow oscillations period ΔV_g is inverse proportional to V_g, independent of coupling strength but relevant to the tube length, this result can be seen from Figure 1 to Figure 2 clearly. The coupling strength can change the ratio of scattered wave part, with the higher terms of the energy dispersion relation, result in subtle structure in conductance curve as seen in Figures 1 and 2. As for the zigzag metallic SWNT electron resonators, since the energy dispersion relations of two channels are always the same, the slow oscillations of conductance will of course not appear (see Fig. 3).

In conclusion, our calculations show that all metallic SWNT resonators have slow oscillations except the zigzag ones, which are independent of the localized states due to the imperfections; The ratio of slow oscillations and fast oscillations is independent of the coupling strength but relevant to the tube length and the gate-voltage; Both rapid

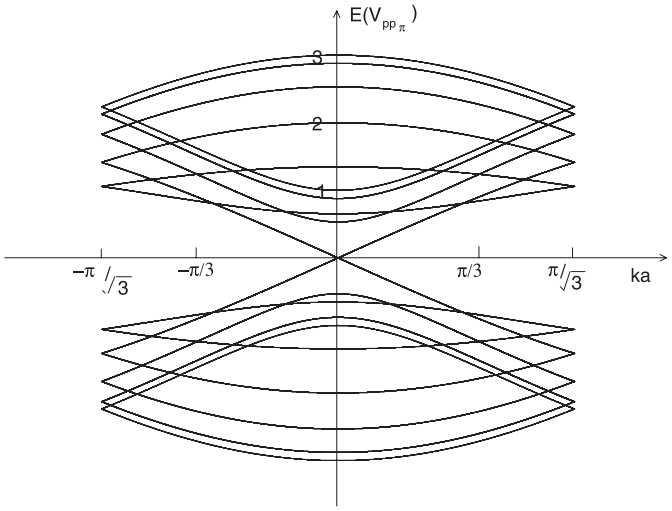

Fig. 5. Energy dispersion relation of (9,0) SWNT around Fermi energy.

and slow conductance fluctuations are quantum interference phenomena, but the former comes from linear terms in the energy dispersion relations of metallic nanotubes, while the latter from nonlinear ones. The SWNT electron waveguide is found to have distinctly different transport behavior depending on whether or not the length of the tube is commensurate with a $(3N + 1)$ rule, with N the number of basic carbon repeat units along the nanotube length.

This work was supported by the Natural Science Foundation of China under Grant No. 10074026, and No. A040108. The authors acknowledge also support from a Grant for State Key Program of China through Grant No. 1998061407.

References

1. S. Iijima, Nature **354**, 56 (1991)
2. R. Saito, M. Fujita, G. Dresselhaus, Phys. Rev. B **46**, 1804 (1992)
3. N. Hamada, S. Sawada, A. Oshiyama, Phys. Rev. Lett. **68**, 1579 (1992)
4. J.M. Mintmire, B.I. Dunlap, C.T. White, Phys. Rev. Lett. **68**, 631 (1992)
5. X. Blase, L.X. Benedict, E.L. Shirley, S.G. Louie, Phys. Rev. Lett. **72**, 1878 (1994)
6. S. Frank, P. Poncharal, Z.L. Wang, W.A. de Heer, Science **280**, 1744 (1998)
7. W. Liang, M. Bockrath, D. Bozovic, J.H. Hafner, M. Tinkham, H. Park, Nature (London) **411**, 665 (2001)
8. J. Kong, E. Yenilmez, T.W. Tombler, W. Kim, H. Dai, Phys. Rev. Lett. **87**, 106801 (2001)
9. P.J. de Pablo, C. Gomez-Navarro, J. Colchero, P.A. Serena, J. Gomez-Herrero, A.M. Baro, Phys. Rev. Lett. **88**, 036804 (2002)
10. A.Bachtold, M.S. Fuhrer, S. Plyasunov, M. Forrero, E.H. Anderson, A. Zettl, P.L. McEuen, Phys. Rev. Lett. **84**, 6082 (2000)
11. J. Nygard, D.H. Cobden, P.E. Lindelof, Nature (London) **408**, 342 (2000)
12. M.B. Nardelli, Phys. Rev. B **60**, 7828 (1999)
13. Jie Jiang, Jinming Dong, D.Y. Xing, Phys. Rev. Lett. **91**, 056802 (2003)
14. L. Chico, V.H. Crespi, L.X. Benrdict, S.G. Louie, M.L. Cohen, Phys. Rev. Lett. **76**, 971 (1996)
15. D.S. Fisher, P.A. Lee, Phys. Rev. B **23**, 6851 (1981)
16. Y. Meir, N.S. Wingreen, Phys. Rev. Lett. **68**, 2512 (1992)
17. S. Datta, *Electronic Transport in Mesoscopic Systems* (Cambridge University Press, Cambridge, 1995)
18. M.P. Lopez-Sancho, J.M. Lopez-Sancho, J. Phys. F **14**, 1205 (1984); M.P. Lopez-Sancho, J.M. Lopez-Sancho, J. Phys. F **15**, 851 (1985)
19. A. Rubio, D. Sanchez-Portal, E. Artacho, P. Ordejon, J.M. Soler, Phys. Rev. Lett. **82**, 3520 (1999)
20. H. Mehrez, J. Taylor, Hong Guo, Jian Wang, C. Roland, Phys. Rev. Lett. **84**, 2682 (2000)
21. D. Orlikowski, H. Mehrez, J. Taylor, Hong Guo, Jian Wang, C. Roland, Phys. Rev. B **63**, 155412 (2001)
22. S. Berber, D. Tomanek, Phys. Rev. B **69**, 233404 (2004)
23. F. Triozon, S. Roche, A. Rubo, D. Mayou, Phys. Rev. B **69**, 121410 (2004)
24. Linfeng Yang, Jiangwei Chen, Huatong Yang, Jinming Dong, Phys. Rev. B **69**, 153407 (2004)